Materials Chemistry and Physics 297 (2023) 127339

Contents lists available at ScienceDirect

Materials Chemistry and Physics

journal homepage: www.elsevier.com/locate/matchemphys

Silver nanoparticle doped graphene-based impedimetric biosensor towards sensitive detection of procalcitonin

Faysal Selimoğlu [a], Bahri Gür [b,*], Muhammed Emre Ayhan [c,**], Fatma Gür [d], Golap Kalita [e], Masaki Tanemura [f], Mehmet Hakkı Alma [g]

[a] Department of Biotechnology, Faculty of Science, Necmettin Erbakan University, Konya, Turkiye
[b] Department of Biochemistry, Faculty of Sciences and Arts, Iğdır University, Iğdır, Turkiye
[c] Department of Metallurgical and Materials Engineering, Faculty of Engineering, Necmettin Erbakan University, Konya, Turkiye
[d] Department of Medical Services and Techniques, Health Services Vocational School, Atatürk University, Erzurum, Turkiye
[e] C's Techno Inc., Co-operative Research Center for Advanced Technology, Nagoya Science Park, Moriyama-ku, Nagoya, 4630003, Japan
[f] Department of Physical Science and Engineering, Nagoya Institute of Technology, Nagoya, Japan
[g] Department of the Biosystems Engineering, Faculty of Agriculture, Iğdır University, Iğdır, Turkiye

HIGHLIGHTS

- The LOD of PCT was determined as 0.55 ngmL^{-1} by impedimetric biosensor applications.
- Reusability of the bio-electrode was determined as 92.5% (I_{pa}) in 20 cycles.
- The storage stability of bio-electrode was determined as 81.8% (I_{pa}) at 24th hours.
- Bio-electrodes suitable for real sample applications were successfully prepared.

GRAPHICAL ABSTRACT

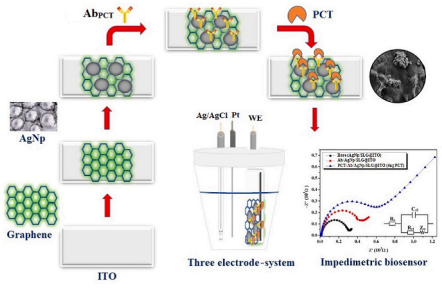

ARTICLE INFO

Keywords:
CVD graphene
Impedimetric biosensor
Procalcitonin
Sepsis
EIS
Thin films

ABSTRACT

In the early detection of sepsis, procalcitonin (PCT) appears to be a highly sensitive biomarker for severe inflammation and infection. A significant interaction between the electrode material to be used in the design of the biosensor and the material to be attached to the surface is of great importance. Here, we demonstrated a silver nanoparticle (AgNp) doped graphene-based sensitive PCT biosensor with low-cost, environmentally friendly materials. Cyclic voltammetry curves showing the reusability of the electrodes obtained were obtained and showed antibody-protein adhesion on the AgNp/SLG@ITO surface. The anodic and cathodic peak currents values after 20 cycles show that these values are suitable even after 20 measurements. Electrochemical impedance spectroscopy (EIS) studies confirmed the effects of PCT on binding events due to increasing concentration at a constant PCT-antibody concentration. The limit of detection (LOD) value of the fabricated PCT/Ab/AgNp/SLG@ITO impedimetric biosensor was determined as 0.55 ngmL^{-1}. The low LOD value can be attributed to the uniform and large surface area of single-layer graphene (SLG) and noble AgNp. The LOD value

* Corresponding author.
** Corresponding author.
E-mail addresses: bahri.gur@igdir.edu.tr (B. Gür), meayhan@erbakan.edu.tr (M.E. Ayhan).

https://doi.org/10.1016/j.matchemphys.2023.127339
Received 9 September 2022; Received in revised form 19 December 2022; Accepted 3 January 2023
Available online 4 January 2023

based on the EIS studies has revealed that the PCT/Ab/AgNp/SLG@ITO impedimetric biosensor can be employed in real samples.

1. Introduction

It is an undeniable fact that technology and modernity bring many diseases along with many conveniences and high-quality living standards. Early diagnosis has always been a major step in the treatment of diseases, and this step will become more important in the near future. Biosensors with high sensitivity are needed in the diagnosis of diseases such as cancer, in the diagnosis of infectious diseases such as Acquired Immune Deficiency Syndrome (AIDS), in the regular monitoring of the quantities of drugs that must be present in the blood for an extended period, in the instantaneous monitoring of substance levels injected into the body during critical medical operations, in the detection of harmful gases in indoor environments, in agriculture, food, animal health, etc. In this context, it is important to develop biomedical products that have multiple detection capabilities to detect specific molecules.

Sepsis is a severe systemic inflammatory response that can result from a bacterial, viral, or fungal infection and remains the primary cause of patient death despite medical advances such as new generation antibiotics or other chemical therapies [1–4]. One of the major limitations in the early diagnosis of sepsis is that its clinical symptoms, including fever, arterial hypotension, and thrombocytopenia, are highly variable, non-specific, and heterogeneous due to the independent cellular metabolic responses that occur during sepsis progression. Such delay in time always leads to an increase in the death of patients. To address these issues, several methods have been developed for the diagnosis of sepsis, including polymerase chain reaction (PCR), electrochemical immunoassay, and surface plasmon resonance. In addition, there is increasing interest in the use of some blood biomarkers, including C-reactive protein (CRP), procalcitonin (PCT), various cytokines, and cell surface markers for the early detection of sepsis. Procalcitonin is widely regarded as a highly sensitive biomarker for severe inflammation and infection. It provides emergency and critical care clinicians with a key aid in diagnosing sepsis [5].

The use of PCT in disease diagnosis has several benefits. First, PCT levels increase rapidly in normal serum within 12–48 h after bacterial invasion. Second, serum PCT is more sensitive and specific than other serum biomarkers, including lactate, CRP, and IL-6. A PCT-based immunoassay has recently been approved by the US Food and Drug Administration (FDA) and is already commercially available [6–12]. Therefore, elevated and circulating PCT levels have been widely investigated as a promising biomarker for the early diagnosis of sepsis, although they have limitations in distinguishing sepsis from other inflammatory conditions. Although high and circulating levels of PCT have limits to distinguish sepsis from other inflammatory conditions, it has been extensively studied as a promising biomarker for early detection of sepsis. Considering this feature, monoclonal, IgG2a Isotype procalcitonin antibody (44D9) was used while preparing the working electrode in biosensor applications for PCT diagnosis within the scope of this study.

The electrochemical biosensor method is widely used for the development of label-free and portable biosensors in many applications. This technique is low cost and provides advantages in terms of fast response time and less maintenance. Therefore, cyclic voltammetry (CV) and electrochemical impedance spectroscopy (EIS) are applied as real-time, label-free, and in situ techniques for monitoring analytes. A biosensor consists of a biosensing material and a transducer and is used to detect biological and chemical active substances. Biosensing materials, including enzymes, antibodies, nucleic acids, cells, tissues, and organelles, can be quantitatively determined with the aid of electrochemical, optical, piezoelectric, thermal, and magnetic devices [13].

Obtaining clear and reliable information on substances collected from living organisms is depends on the sensitivity of biological sensors that convert biological signals to electrical signals. The amount of substance taken is usually measured in milligrams/liter or millimoles/liter, due to their very low concentrations. Micro/nano biosensors need to be developed in order to make accurate and sensitive measurements because the measured substances are in micro and nano dimensions. It is seen that nano biosensors are one million times more sensitive than conventional biosensors because they can detect at nanomole/liter or picomole/liter levels [14–19].

Graphene is one atom thick and with a honeycomb-shaped hexagonal crystal structure promising carbon material in sensor applications due to its high reactivity, high surface area, and biocompatibility. Two-dimensional (2D) materials, especially graphene, have recently become of interest in the development of sensors and detector-like devices. Zhang and Cui have developed a flexible graphene-based cancer sensor for the detection of low-concentration specific prostate antigens using the layer-by-layer self-assembly technique [20]. Kwon et al. developed a flexible biosensor using few-layer graphene synthesized by the chemical vapor deposition method [21]. Kwak et al. have manufactured a flexible glucose sensor in the graphene/graphene oxide FET structure by functionalizing the glucose oxidase enzyme [22]. Many researchers have studied a graphene-based biosensor containing functional groups for the detection of *Escherichia coli* bacteria in the human intestine [23–29]. Basu et al., on the other hand, succeeded in producing a graphene-based *Escherichia coli* biosensor on a flexible acetate substrate using a low-cost method without using any functional groups [30]. Furthermore, studies of graphene-based electronic and photonic biochemical sensors have been conducted for DNA, RNA, and cell structures [31–34]. In addition, applications of highly sensitive graphene-fiber hybrid biochemical sensors are possible with flexible graphene films coated with fiber optic [35]. B.C.Yao et al. developed a graphene-based D-shaped polymer fiber Bragg grid (GDPFBG) biosensors to detect human red blood cell (RBC) concentration [36].

In this study, bio-electrodes design and production with AgNp/SLG@ITO hybrid structure, which provides a nano-molar measurement for accurate, clear, and fast detection of PCT biomarker, and impedimetric biosensor applications were carried out. The developed 2D nano materials-based impedimetric biosensor application has the advantages in: (i) High sensitivity and reliable analysis test results can be obtained. (ii) Can be possible to perform faster analyzes compared to traditional biosensors. (iii) Since the consumption of consumables can be lower, it can be an economical product. (iv) It can be an environmentally friendly product in terms of waste amount and production technique. (v) It can be a product with commercialization potential.

2. Experimental

2.1. Chemicals and apparatus

Polystyrene, poly (methyl methacrylate) (PMMA), iron (III) nitrate nonahydrate solution [$Fe(NO_3)_3 9H_2O$] (99.95%), silver nanoparticles (AgNps) and procalcitonin protein (PCT) were purchased from Sigma-Aldrich. Cu foil (thickness 20 μm, 99.9% purity) was purchased from Nilaco Corporation. Procalcitonin Antibody (44D9) (Ab) was purchased from Novus Biologicals.

2.2. Synthesis of single-layer graphene (SLG) and graphene transfer

High-quality SLG synthesis was performed similarly to the previous report using low-pressure chemical vapor deposited (LP-CVD) system [37]. The synthesized SLGs on the Cu foils were coated with a low

average molecular weight (AMW) of ~15.000 (by GPC) PMMA/acetone solution by spin coating. Due to a low AMW, PMMA solution shows a lower doping level and enhanced carrier mobility, resulting in a cleaner surface with negligible residues [38]. PMMA-covered SLG sheets were dried at 80 °C for 15 min. To etch the Cu foils the dried samples were dipped in a diluted [$Fe(NO_3)_3$ $9H_2O$] solution overnight. Obtained PMMA/SLG sheets were washed with deionized water (DIW) and soaked in a diluted HCl solution to remove [$Fe(NO_3)_3$ $9H_2O$] residual. PMMA/SLG sheets were washed with DIW and transferred onto indium tin oxide (ITO) substrates. ITO substrates were immersed in isopropyl alcohol, ethyl alcohol, and deionized water for 15 min to remove residue, dust, and impurities from the surface layer before the transfer proses [39,40]. The resulting PMMA/SLG@ITO stack layers were dried in an oven at 80 °C for 15 min. Then the PMMA layers were removed from the SLG surface by dipping in acetone and isopropyl alcohol. Finally, SLG@ITO films were successfully obtained after the transfer procedure.

2.3. Fabrication of AgNp/SLG@ITO impedimetric biosensor applications for PCT detection

Fig. 1 represents the schematic diagram of the PCT impedimetric biosensor design. AgNps (60 nm) were decorated on the SLG@ITO films by drop-casting and AgNp/SLG@ITO electrode structures were obtained for the PCT biosensor device. The pre-functionalized AgNp/SLG@ITO electrodes were dried with N_2 gas for a few seconds. After these steps, the electrodes and the voltammetric cells were combined and incubated for 1 h at +4 °C to immobilize the procalcitonin antibody onto the AgNp/SLG@ITO electrodes. The cell was washed with PBS (pH 7.4) and then again with DIW to remove the unbound procalcitonin antibody. Then, 2 μL of pure procalcitonin proteins were loaded into the antibody immobilized cell and incubated at +4 °C for 1 h. Cells were washed with PBS and DIW, respectively, to remove unbound proteins.

2.4. Crystallographic and morphological characterizations

Raman analysis of synthesized SLG materials was carried out with Renishaw-INVIA Reflex Raman spectrometer. Field emission scanning electron microscope (FESEM) images and energy-dispersive X-ray (EDX) spectrum were collected with Zeiss Gemini. Fourier Transform Infrared Spectrometer (FT-IR) through a 500–4000 nm range were collected with Thermo Scientific-Nicolet iS20.

2.5. Amperometric measurement method: Cyclic voltammetry (CV) and electrochemical impedance spectroscopy (EIS) measurements

CV and EIS measurements were performed using an electrochemical analyzer (Gamry potentiostat) connected to a computer data analysis system. A three-electrode system, including a working electrode, platinum counter electrode, and Ag/AgCl reference electrode was used for electrochemical measurements. These analyzes were performed in a phosphate buffer solution (PBS) containing 4 mM Ferro/ferricyanide. CV measurements for PCT-containing electrodes (PCT/Ab/AgNp/SLG@ ITO) were recorded from −0.4 V to +0.4 V against an Ag/AgCl reference electrode at a scanning rate of 20 mV/s. CV measurements for the bare electrode (AgNp/SLG@ ITO) and the antibody-containing electrode (Ab/AgNp/SLG@ ITO) were carried out in the range of −0.5 V to +0.5 V. EIS measurements were performed using an alternating voltage of 10 mV in the frequency range 10 Hz-10 kHz with a DC potential of 0.2 V. In all experimental studies, the repeatability characteristic (n = 3) was tested for the determined concentrations.

3. Results and discussions

3.1. Crystallographic and morphological characterizations of AgNp/SLG-based electrodes

Synthesis of graphene and crystallographic analysis were investigated by Raman spectroscopy studies. Fig. 2a shows the Raman spectra of the fabricated carbon material fabricated by the LP-CVD method. The specific peaks in the Raman spectra were observed in ~1587 corresponding to G (sp^2 hybridizations) peak and a strong peak at ~2680 cm^{-1} corresponding to the 2D (second-order, also called G′) peak. The strong and sharp peak at the G′ band and the ratio of $I_{G'}/I_G$ about 2 indicate that synthesized materials are SLG. In addition, an insignificant defect-related peak at ~1343 cm^{-1} corresponding to D (sp^3 hybridizations) peak demonstrates that synthesized SLGs are high crystallinity carbon materials.

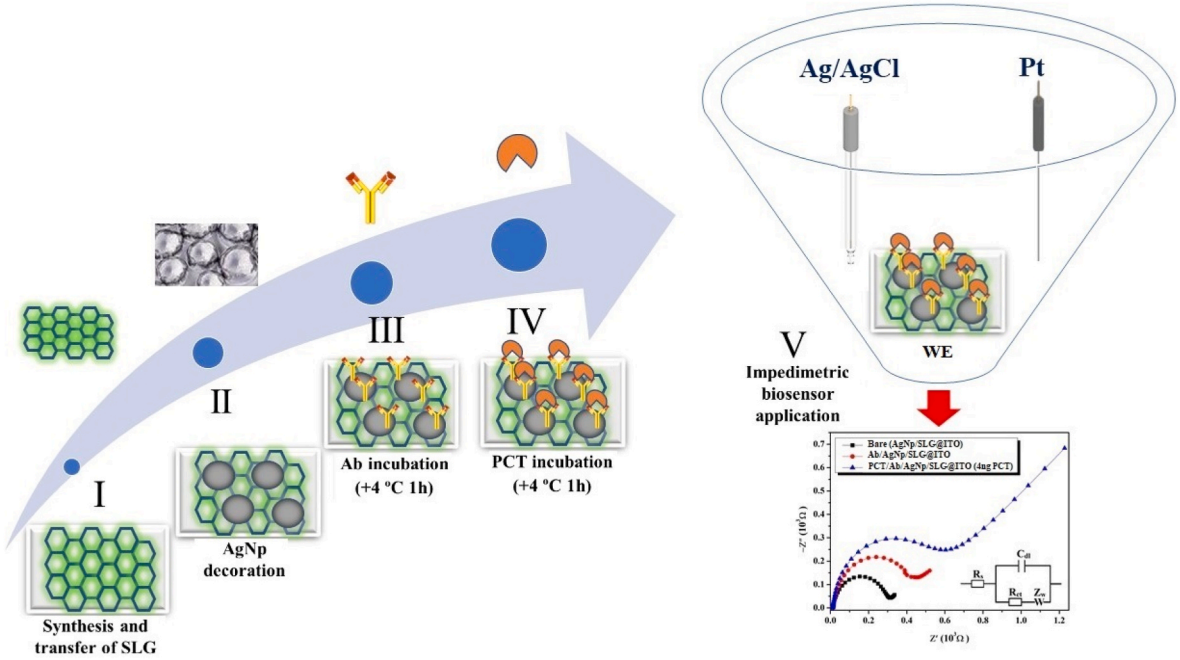

Fig. 1. Schematic illustration of AgNp/SLG@ITO impedimetric biosensor application.

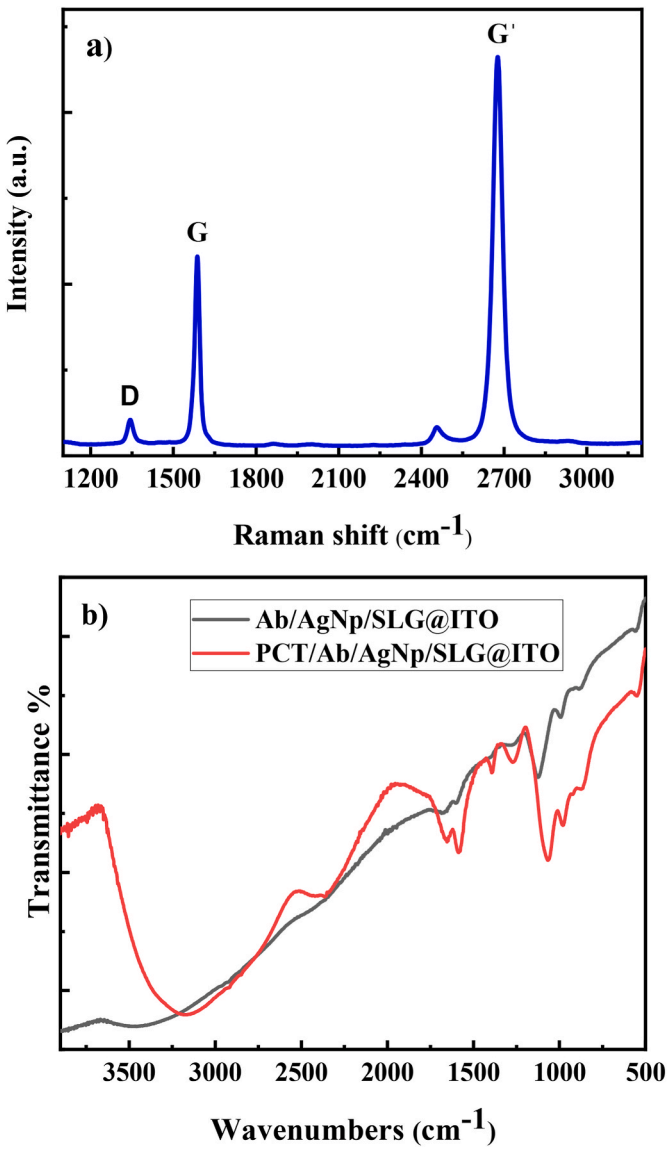

Fig. 2. (a) Raman spectra of synthesized SLG **(b)** FT-IR spectra of fabricated Ab/AgNp/SLG@ITO and PCT/Ab/AgNp/SLG@ITO electrodes.

The chemical composition of the electrode surfaces and binding of Ab_{PCT} with the AgNps decorated SLG was investigated using FT-IR studies. Fig. 2b shows the FT-IR spectra of Ab/AgNp/SLG@ITO and PCT/Ab/AgNp/SLG@ITO. All spectra show a broad peak in the range of 3500–1500 cm^{-1}. As seen in Fig. 2b, the peaks for Ab/AgNp/SLG@ITO correspond to the carboxy, epoxy, alkoxy, etc. After incubation of PCT protein, these peaks were shifted as follows. The assignation (cm^{-1}) for Ab/AgNp/SLG@ITO: 1693.7 and 1684.91 C═O stretching; 1126.44 C–O stretching (epoxy); 993.28 C–O stretching (alkoxy); 3457.38 O–H (stretching of the C–OH). The assignation (cm^{-1}) for PCT/Ab/AgNp/SLG@ITO: 980 and 1066.47 epoxy vibration; 1272.86 C–O vibration of the C–OH; 1393.71 O–H vibration of the C–OH; 1585.96 –COO stretching 1653.81 C═O stretching; 3163.87 O–H (stretching of the C–OH) [41,42]. The accomplishment of incubation of PCT was demonstrated in the FT-IR spectrum of Ab/AgNp/SLG@ITO and PCT/Ab/AgNp/SLG@ITO electrodes with the changes in the peak positions that were observed in the obtained spectra.

Fig. 3 shows the FESEM images taken for the antibody-doped and PCT-doped electrodes. After the ITO surface was coated with AgNp@SLG, it became an effective matrix for antibody immobilization. Upon immobilization of the antibody, the structures shown in Fig. 3a show obvious antibody aggregation. Comparing Fig. 3a and b, a varying morphology was obtained depending on the incubation of the PCT protein. Fig. 3b shows a clear variation in the electrode surface topography as a result of PCT attaching to Ab compared to Fig. 3a. These results demonstrated successful binding of the antibody (Fig. 3b). As seen in Fig. 3b, the interaction between Ab and PCT increased surface roughness. In conclusion, FESEM morphology results proved the accuracy of CV and EIS.

3.2. *Electrochemical characterization of AgNp/SLG-based electrodes*

The prepared bare (AgNp/SLG@ITO), Ab/AgNp/SLG@ITO, and PCT/Ab/AgNp/SLG@ITO electrodes were characterized electrochemically to evaluate the oxidation and reduction potential of 4.0 mM Fe $(CN)_6^{3-}$ in a pH 7.4 PBS medium. CV measurements taken at a scanning rate of 20 mV/s for the prepared bare electrodes are shown in Fig. 4. It was understood that no anodic and cathodic peak currents were observed in the CV curve given to the bare electrode in Fig. 4, however anodic and cathodic currents emerged for the Ab/AgNp/SLG@ITO electrode obtained as a result of incubation of the PCT antibody. The CV curve obtained from the probe electrode (PCT/Ab/AgNp/SLG@ITO) prepared as a result of the incubation of the PCT protein showed that anodic and cathodic peak currents were obtained depending on the antibody-protein interaction, which is in accordance with the studies previously reported in the literature [12,43].

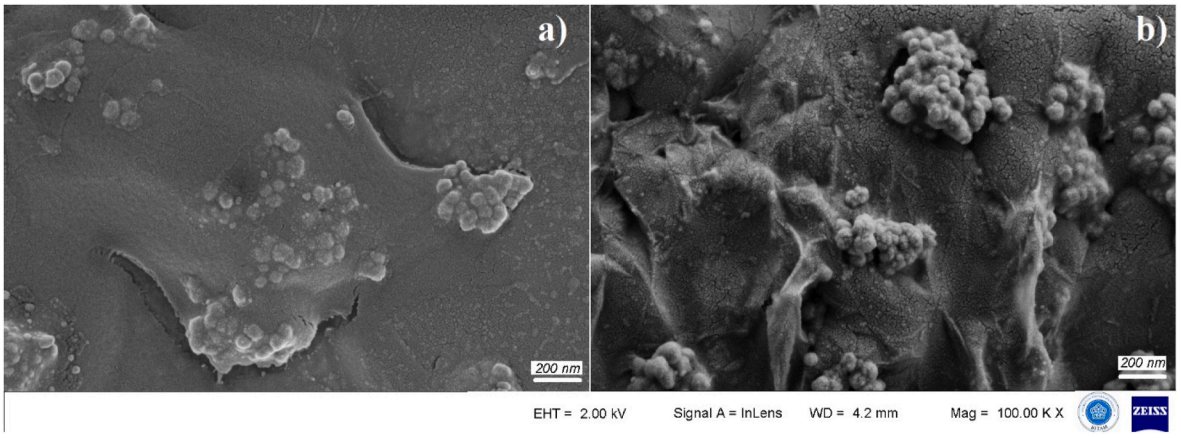

Fig. 3. FESEM images of Ab and PCT/Ab covered on AgNp/SLG@ITO electrode. **(a)** FESEM results at 200 nm scale bar for Ab/AgNp/SLG@ITO electrode **(b)** FESEM results at 200 nm scale bar for PCT/Ab/AgNp/SLG@ITO electrode.

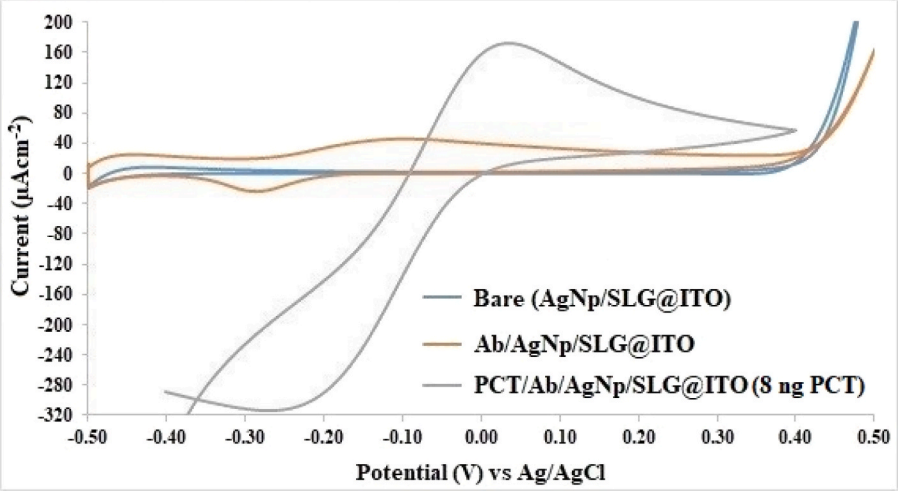

Fig. 4. Cyclic voltammograms of bare, Ab/AgNp/SLG@ITO, and PCT/Ab/SLG/AgNp/@ITO electrodes (8 ng mL^{-1} PCT, scan rate: 20 mVs^{-1}).

It was observed that with the increase of PCT concentration (from 2.0 ng mL^{-1} to 25.0 ng mL^{-1}) on the Ab/AgNp/SLG@ITO electrode surface, there was an increase in the anodic and cathodic peak currents due to protein-antibody interaction (Fig. 5a). This increase observed in Fig. 5a shows that CV studies for biosensor applications are appropriate. When Fig. 5a is examined, higher oxidation and reduction peak currents were observed in PCT/Ab/AgNp/SLG@ITO electrodes compared to bare and Ab/AgNp/SLG@ITO electrodes in the CV curves obtained in the electrolyte solution containing $Fe(CN)_6^{3-}$.

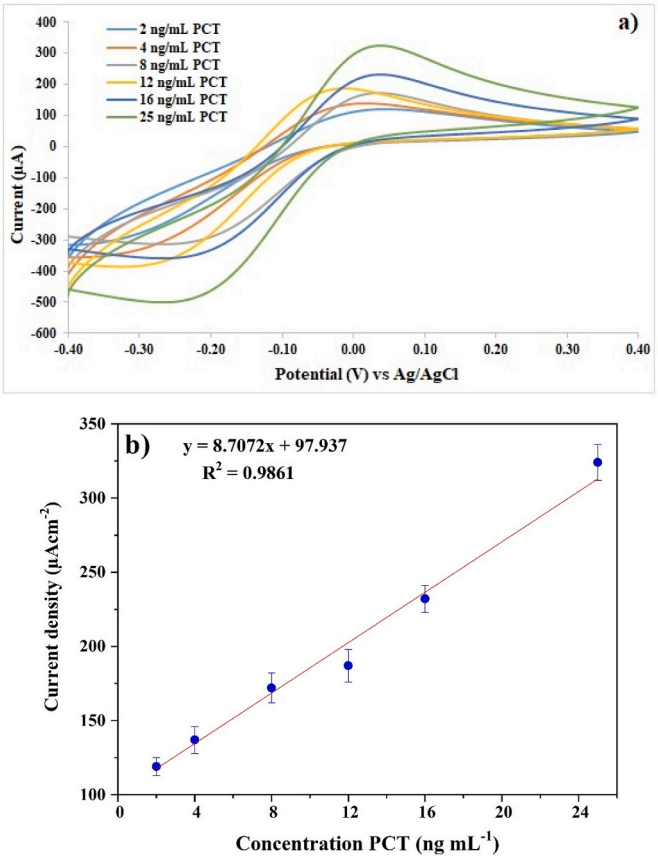

Fig. 5. (a) CV curves of PCT/Ab/AgNp/SLG@ITO electrodes in the potential range of −0.4 V to +0.4 V and PCT concentration range of 2–25 ng mL^{-1} (Scan speed: 20 mVs^{-1}) **(b)** Anodic calibration curve derived from CV.

The intensity of these peak currents increased in direct proportion to the increasing PCT concentration [44]. Based on the anodic peak formations observed in the CV curves obtained in Fig. 5a, the performances of the prepared PCT/Ab/AgNp/SLG@ITO electrodes were verified with the anodic calibration curve and are shown in Fig. 5b.

The lowest concentration detected and measured is known as the limit of detection (LOD) and the limit of quantitation (LOQ), respectively. The sensitivity of the sensor is an important parameter that shows how sensitive the electrode produced for electrochemical methods is in a sensor study. Sensitivity, LOD, and LOQ values were calculated with the following equations using data from the anodic calibration curve given in Fig. 5b [45].

$$\text{sensitivity} = \frac{S}{\text{electrode surface area}}, \text{LOD} = \frac{3\sigma}{S}, \text{and LOQ} = \frac{10\sigma}{S}$$

Where σ is the standard deviation of the curve obtained from electrochemical studies for the PCT-free electrode (Ab/AgNp/SLG@ITO) and S is the slope of the calibration graph.

Fig. 5a and b shows the CV curves obtained depending on the working electrodes prepared at different PCT concentrations and the anodic calibration curve obtained from these curves. As seen in Fig. 5a, the anodic and cathodic current densities increase linearly with increasing PCT concentration. LOD, LOQ, and sensitivity values of the prepared PCT/Ab/AgNp/SLG@ITO biosensors were calculated considering the anodic calibration curve and were determined as 0.57 ng mL^{-1}, 1.89 ng mL^{-1}, and 5.80 $\mu Ang^{-1}mLcm^{-2}$, respectively. The equation for the anodic calibration curve is obtained as J (μAcm^{-2}) = $8.7072C_{PCT} + 97.937$ with a correlation coefficient of 0.9861.

A sensor prepared for electrochemical analysis of the PCT by the CV method is expected to have superior properties in terms of high stability, reliability, and reusability. Therefore, the repeatability (n = 3) and reusability properties (n = 20 cycles) of the proposed PCT sensor based on Ab/AgNp/SLG@ITO were tested. 20 cycles were performed for the biosensor containing PCT at a concentration of 8 ng mL^{-1} and the obtained voltammograms were shown in Fig. 6a. In addition, the storage stability properties of the PCT/Ab/AgNp/SLG@ITO bioelectrode prepared after incubation at +4 °C for 1 h were clarified by CV studies and shown in Fig. 6b. In storage stability studies, CV measurements were performed immediately (after PCT incubation) once the PCT/Ab/AgNp/SLG@ITO bioelectrodes were prepared. Thereafter, the prepared bioelectrodes were stored for 24 h at +4 °C in a closed, dust-tight environment and the CV measurements were repeated.

Other factors affecting the long-term performance capability of the prepared biosensor are the sensor stability parameter and storage stability parameter. The proposed Ab/AgNp/SLG@ITO sensor probe with

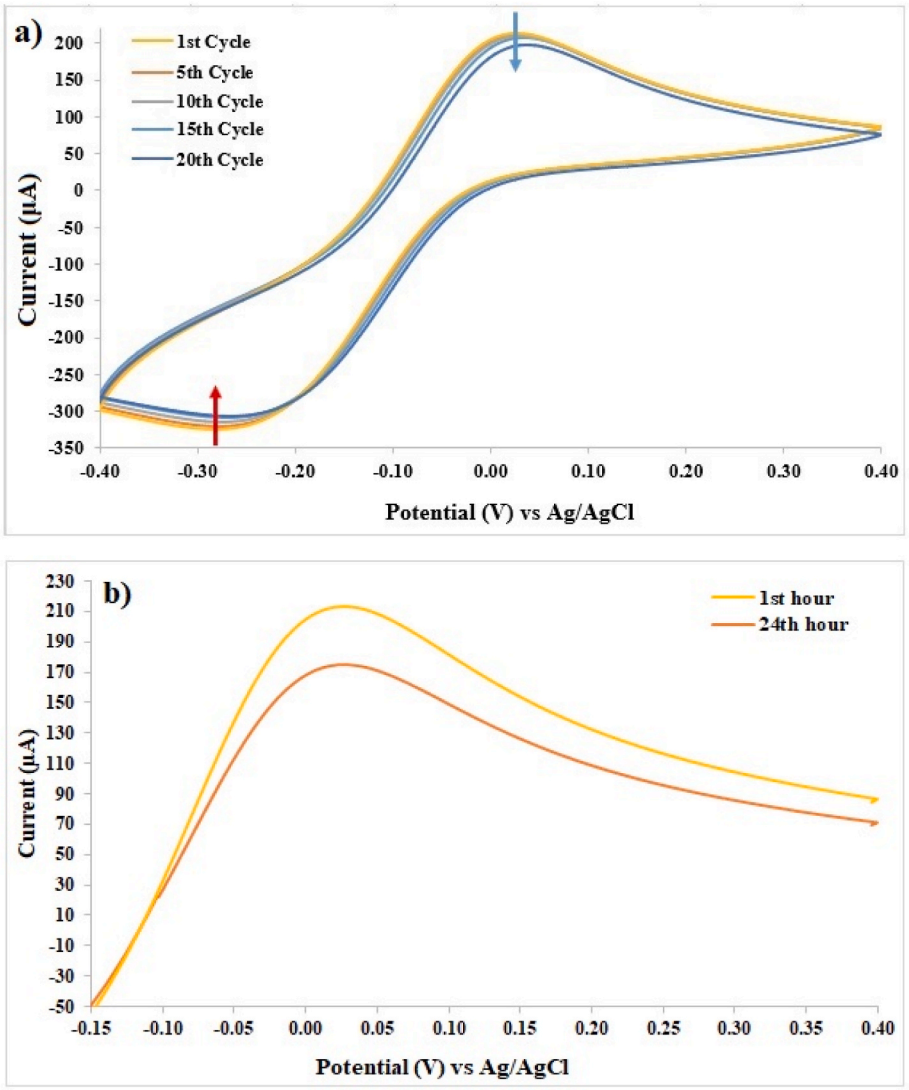

Fig. 6. **(a)** Sequential CV curves of the PCT/Ab/AgNp/SLG@ITO electrode at a potential range of −0.4 V to +0.4 V and a PCT concentration of 8 ng mL-1 (Scan speed: 20 mVs^{-1}) **(b)** Storage stability of PCT/Ab/AgNp/SLG@ITO electrode (8 $ngmL^{-1}$ PCT), (24 h, +4 °C storage).

phosphate buffer solution in PBS medium at pH 7.4 was found to be stable in CV for 20 cycles under the same conditions. Considering Fig. 6 a, after 20 cycles, the anodic peak current (I_{pa}) peak point decreased from 214 µA to 198 µA, while the cathodic peak current (I_{pc}) peak point decreased from 323 µA to 304 µA. The decreases of 92.5% and 94.11% observed in I_{pa} and I_{pc} values, respectively, after 20 cycles show that these values are appropriate even after 20 measurements and the electrode stability used in the PCT biosensor prepared according to these results is excellent. On the other hand, the obtained CV measurements on the storage stability of the sensor showed that the peak Ipa value decreased from 214 µA to 175 µA (81.8%) after 24 h of storage (Fig. 6b). From the stability and storage stability values obtained, it can be concluded that the recommended PCT/Ab/AgNp/SLG@ITO electrode can operate efficiently for a long period of time at +4 °C in a closed, dust-tight environment [44].

3.3. Analytical performances of the impedimetric biosensors

An impedimetric biosensor was developed to measure the charge conductivity and capacitance changes on the PCT/Ab/AgNp/SLG@ITO sensor surface, which is formed by the selective binding of the target protein PCT to the antibody (Ab_{PCT}) incubated on the AgNp/SLG@ITO electrode surface. Here, Electrochemical Impedance Spectroscopy (EIS) technique was used in addition to the CV technique to investigate the electrochemical properties of the incubation steps in preparation of the impedimetric sensor associated with varying PCT concentrations in the analyte for PCT detection. Additionally, EIS was used to measure impedance changes in electrodes due to modifications. Similar to the CV technique, 4 mM $Fe(CN)6^{3-}$ was used as a redox-active probe to observe the electron transfer between the electrolyte and the ITO electrode surface. With this probe, modifications made depending on Ab_{PCT} incubation and PCT incubation at different concentrations were followed.

EIS technique is used as a sensitive and convenient technique to monitor the impedance change due to the modification of the prepared biosensor [12,46]. In addition to the interactions between the prepared electrode surface and the electrolyte solution, the interactions of these molecules with the electrode surface as a result of Ab and PCT incubation were explained by the EIS technique. The impedance spectra of the electrodes prepared in this study were performed at an AC potential of 0.2 V using an alternating voltage of 10 mV in the frequency range of 10 Hz to 10 kHz and are shown in Fig. 7.

The graph obtained when high-frequency to low-frequency currents pass through the electrode surface is a Nyquist curve. In the absence of any change in the electrode surface, this curve occurs as a semicircle.

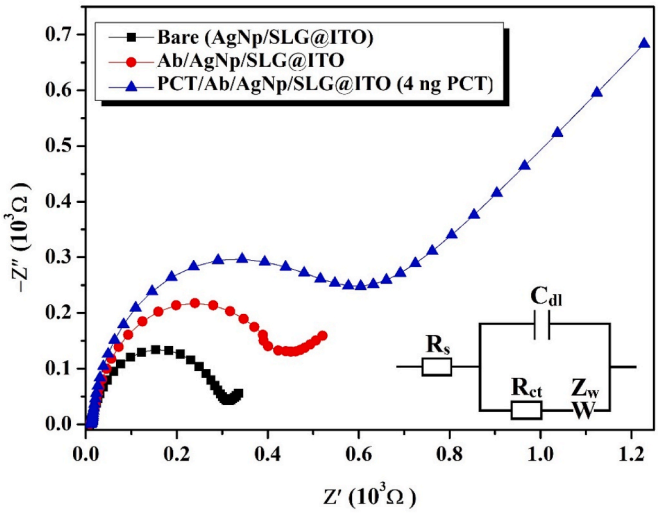

Fig. 7. EIS Nyquist plot of PCT impedimetric biosensor construction steps. The inset presents a Randles circuit (an equivalent electrical circuit).

Events on the electrode surface cause linear changes at the end of this semicircle (Fig. 7). The X-axis of the curve gives information about the resistance of the electrode, while the Y-axis gives information about the capacitance of the electrode. In this study, the prepared ITO electrodes were coated with AgNp and graphene, which are capacitive anode materials for PCT detection, and were shown as double layer capacitance (C_{dl}). There is also the resistance defined as the charge transfer resistance (R_{ct}), and this resistance is the resistance of the electricity passing between the interface and the electrode. Another resistance observed in the circuit is the solution resistance (R_s). Finally, the Warburg (W) impedance is an equivalent electrical circuit component that models the diffusion process.

Since EIS studies are performed at high frequencies (10 kHz), the impedance is very low. Therefore, the current passes through R_s and continues through the capacitor. Such cells are called Randles circuits and are ideal for biosensor applications. Considering Fig. 7, the circuit consists of solution resistance (R_s), charge transfer resistance (R_{ct}), double layer capacitance (C_{dl}), and Warburg element (W). While R_s are observed at high frequencies, in addition to R_s at very low frequencies, a diffusion-induced (from solution to the electrode) charge transfer resistance (R_{ct}) is observed together. On the other hand, at very low frequencies, the diffusion effect from the solution to the electrode causes Z_w. R_s and W reflect the property of the solution, while together with C_{dl}, R_{ct} depends on the electrical property at the electrode-electrolyte interface.

The linear part of the Nyquist plot obtained from the electrode containing PCT in Fig. 7 appeared as a linear straight line at 45° to the real axis (Z'). This corresponds to lower frequencies representing the electron transfer and emission process. The linearity in the EIS spectrum for the PCT/Ab/AgNp/SLG@ITO electrode also indicates that the electron transfer of $[Fe(CN)6]^{-3}$ is faster and the electrode surface is expanded due to AgNp/SLG nanostructures on the surface [47]. The diameter of the semicircle, which occurs at higher frequencies, is attributed to the resistance of electron transfer. By analyzing these semicircles, the properties of the electrolyte and the prepared PCT electrodes were investigated [46,47].

In addition to CV studies, EIS studies were also carried out in order to determine the quantitative properties of the prepared PCT biosensor. Ab_{PCT} antibody (2.0 μg mL^{-1}) concentration was first incubated on AgNp/SLG@ITO electrodes and PCT was applied on these electrodes at concentrations ranging from 2 to 25 $ngmL^{-1}$, respectively. Then, the impedance changes in electrodes containing different concentrations of PCT prepared were measured by EIS before and after incubation with

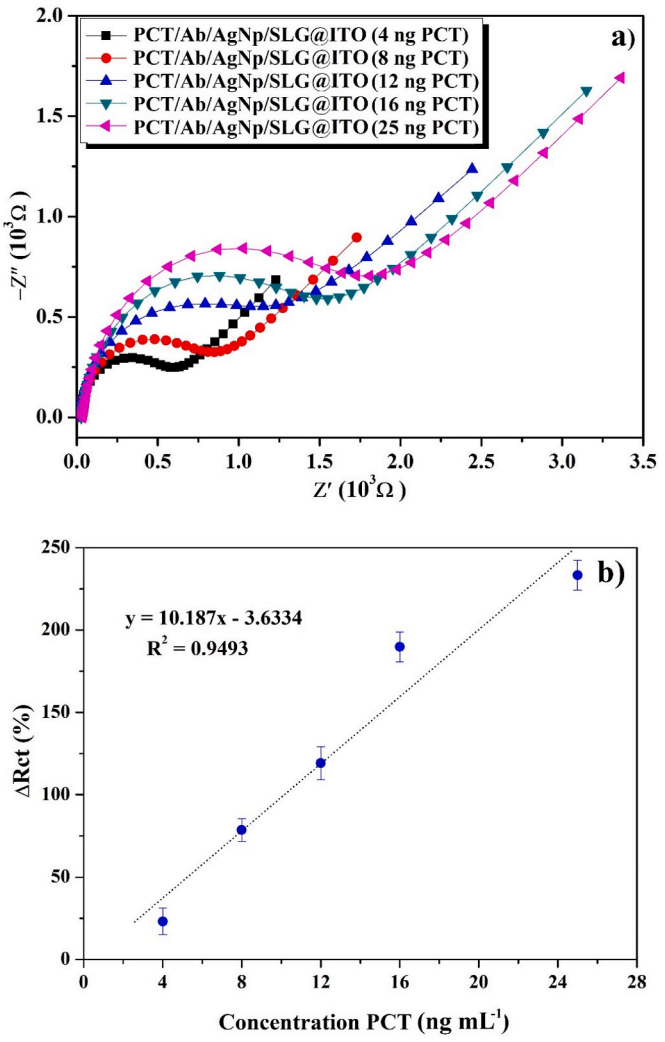

Fig. 8. **(a)** Nyquist plots of the impedimetric biosensor incubated at increasing PCT concentrations (4 ng–25 ng) **(b)** Calibration curve of the developed impedimetric biosensor.

PCT and are given in Fig. 8. As shown in Fig. 8a, a dynamic change in both electrode resistance (Z') and electrode capacitance (Z") was observed depending on the increasing PCT concentration in impedance. With this method, the effects of PCT on bindings due to increasing concentration at a constant Ab_{PCT} concentration were also confirmed. The calibration curve of the biosensor, which was developed with the help of Nyquist graphs of the impedimetric biosensor obtained due to the increasing PCT concentrations given in Fig. 8a, was obtained with the following equation [12,48]. LOD, LOQ, and sensitivity values of the PCT biosensor were calculated as described in the CV method [45,49].

$$\Delta Rct = \frac{Rct(PCT) - Rct(Ab)}{Rct(Ab)} * 100$$

In the equation, the charge transfers value R_{ct} (PCT) represents the value of the semicircle diameter in the EIS curve obtained as a result of the interaction of Ab_{PCT} and PCT. R_{ct} (Ab) is the charge transfer value obtained after incubation of Ab_{PCT} on the surface of AgNp/SLG.

Fig. 8a shows Nyquist plots of the PCT impedimetric sensor incubated at constant Ab_{PCT} concentration. As seen in Fig. 8a, both charge transfer resistance values and capacitance values of the electrodes increased depending on the increasing PCT concentration. Impedance measurements present the signal as a function of frequency at a constant potential and involve the application of a small sinusoidal AC voltage

probe and determining the current response [50,51]. Impedance measurements related to biosensor studies are generally expected to comply with the Randles equivalent circuit shown in Fig. 7. Here Rct is the load transfer resistance. Prepared PCT impedimetric biosensors detect a change in one of these equivalent circuit parameters due to analyte binding. In our study, PCT proteins were most sensitively detected through the increase in load transfer resistance due to increasing protein concentration [50,52,53]. In Fig. 8a, it was observed that Rct increased with increasing PCT values, which was consistent with the literature [12,47,50].

The calibration curve of the impedimetric biosensor in Fig. 8b shows the linear relationship between ΔR_{ct} and increasing PCT concentration. The linear regression equation for the calibration curve given in Fig. 8b was determined as $y = 10.187x - 3.6334$ and the correlation value (R^2) is 0.9493.

LOD, LOQ, and sensitivity values of the prepared PCT/Ab/AgNp/SLG@ITO biosensor were determined as 0.55 $ngmL^{-1}$, 1.82 $ngmL^{-1}$, and 6.79 $ng^{-1}mLcm^{-2}$, respectively, taking into account the calibration curve. These calculated values are consistent with the values obtained based on CV studies. The low LOD value obtained for the PCT/Ab/AgNp/SLG@ITO biosensor can be attributed to the large surface area of graphene and AgNp used in the biosensor preparation. An increase in the electrode surface area causes an increase in the number of antibodies bound to the surface and, accordingly, more interaction with PCT [46,54]. As determined in the literature, plasma PCT levels are very low in healthy individuals (<0.1 ng mL^{-1}) [55,56]. A concentration of ≤ 0.2 $ngmL^{-1}$ has been reported as a useful reference range to rule out sepsis and systemic inflammation. Plasma levels of ≥ 0.5 $ngmL^{-1}$ are interpreted as abnormal as the cutoff value for the diagnosis of sepsis in the patient. In this case, a bacterial infection is predicted and the patient is considered to have sepsis [56–58]. The calculated LOD value (0.55 $ngmL^{-1}$) based on the EIS studies given in Fig. 8 has shown that the prepared PCT/Ab/SLG/AgNp/@ITO biosensor can be applied to real sample studies in accordance with the literature studies [59].

The recently demonstrated PCT biosensors and their LOD values are given in Table 1. Although LOD concentration values at the $pgmL^{-1}$ level were obtained in previous studies, the fact that our biosensors produced by the green synthesis method are cheap, easy and fast to apply, and most importantly, obtaining a PCT detection value of 0.50 $ngmL^{-1}$ for real sample studies can be considered as the advantageous aspects of our study.

4. Conclusion

Obtaining clear and reliable information about the PCT biomarker depends on the sensitivity of the sensors that convert biological signals into electrical signals. With the developed PCT/Ab/AgNp/SLG@ITO impedimetric biosensor, lower LOD, LOQ, and higher sensitivity values were obtained for PCT. CV test results demonstrated that the reusability of the electrodes obtained by antibody and protein incubation was obtained and showed antibody and protein adhesion on the AgNp/SLG@ITO electrode surface. EIS studies confirmed the effects of PCT on binding events due to increasing concentration at a constant Ab_{PCT} concentration. LOD, LOQ, and sensitivity values of the impedimetric biosensor were consistent with the values obtained based on the CV studies. The obtained LOD value (0.55 ng mL^{-1}) based on the EIS studies has revealed that the impedimetric biosensor can be employed in real sample studies. These nano material-based biosensors, which are produced for the early diagnosis of sepsis, are also very advantageous in terms of the long usage time in biosensor applications due to their long electrode storage stability, using cheap and environmentally friendly materials and methods.

CRediT authorship contribution statement

Faysal Selimoğlu: Methodology, Writing – original draft. **Bahri Gür:** Conceptualization, Methodology, Writing – original draft, Software. **Muhammed Emre Ayhan:** Conceptualization, Project administration, Methodology, Formal analysis, Writing – original draft. **Fatma Gür:** Conceptualization, Methodology, Formal analysis, Writing – original draft. **Golap Kalita:** Resources, Writing – original draft. **Masaki Tanemura:** Resources, Supervision, Writing – original draft. **Mehmet Hakkı Alma:** Supervision, Visualization.

Table 1
Comparison of the recently reported PCT biosensor.

Detection method	LOD	Transducer	Reference
Electrochemical immunosensor	0.002 pg mL^{-1}	Electrochemical	[60]
Sandwich-type electrochemical immunosensor	1.23 pg mL^{-1}	Electrochemical	[61]
Label-free electrochemical immunosensor	16.70 pg mL^{-1}	Differential Pulse Voltammetry (DPV) and Amperometric	[62]
EIS	12.5 ng mL^{-1}	Electrochemical	[12]
Sandwich strategy-mediated immunosensor	0.081 ng mL^{-1}	Label-free Imaging Ellipsometry (IE)	[63]
One-step sandwich CLIA EISA	0.0075 ng mL^{-1}	Chemiluminescence Immunoassay	[64]
EIS	0.55 ng mL^{-1}	Electrochemical	Presented work

Declaration of competing interest

The authors declare that they have no known competing financial interests or personal relationships that could have appeared to influence the work reported in this paper.

Data availability

No data was used for the research described in the article.

Acknowledgment

This research has been supported by the Scientific Research Projects Coordination Unit at Necmettin Erbakan University with Grant No:201219006. We thank the Turkish Academy of Sciences (TÜBA) for their support.

References

[1] M. Kemmler, U. Sauer, E. Schleicher, C. Preininger, A. Brandenburg, Biochip point-of-care device for sepsis diagnostics, Sensor. Actuator. B Chem. 192 (2014) 205–215, https://doi.org/10.1016/j.snb.2013.10.003.
[2] J. Cohen, C. Brun-Buisson, A. Torres, J. Jorgensen, Diagnosis of infection in sepsis: an evidence-based review, Crit. Care Med. 32 (2004) S466–S494, https://doi.org/10.1097/01.ccm.0000145917.89975.f5.
[3] T. Rowland, H. Hilliard, G. Barlow, Procalcitonin: potential role in diagnosis and management of sepsis, Adv. Clin. Chem. 68 (2015) 71–86, https://doi.org/10.1016/bs.acc.2014.11.005.
[4] D. Anand, S. Das, S. Bhargava, L.M. Srivastava, A. Garg, N. Tyagi, S. Taneja, S. Ray, Procalcitonin as a rapid diagnostic biomarker to differentiate between culture-negative bacterial sepsis and systemic inflammatory response syndrome: a prospective, observational, cohort study, 218. e217-218, J. Crit. Care 30 (2015), https://doi.org/10.1016/j.jcrc.2014.08.017. e212.
[5] K.L. Becker, R. Snider, E.S. Nylen, Procalcitonin assay in systemic inflammation, infection, and sepsis: clinical utility and limitations, Crit. Care Med. 36 (2008) 941–952, https://doi.org/10.1097/CCM.0B013E318165BABB.
[6] H. Li, Y. Sun, J. Elseviers, S. Muyldermans, S. Liu, Y. Wan, A nanobody-based electro chemiluminescent immunosensor for sensitive detection of human procalcitonin, Analyst 139 (2014) 3718–3721, https://doi.org/10.1039/C4AN00626G.
[7] G. Sener, E. Ozgur, A.Y. Rad, L. Uzun, R. Say, A. Denizli, Rapid real-time detection of procalcitonin using a microcontact imprinted surface plasmon resonance biosensor, Analyst 138 (2013) 6422–6428, https://doi.org/10.1039/C3AN00958K.

[8] P.M. Krämer, M. Keß, E. Kremmer, S. Schulte-Hostede, Multi-parameter determination of TNFα, PCT and CRP for point-of-care testing, Analyst 136 (2011) 692–695, https://doi.org/10.1039/C0AN00699H.

[9] S. Kibe, K. Adams, G. Barlow, Diagnostic and prognostic biomarkers of sepsis in critical care, J. Antimicrob. Chemother. 66 (2011) ii33–ii40, https://doi.org/10.1093/jac/dkq523.

[10] B.M. Tang, G.D. Eslick, J.C. Craig, A.S. McLean, Accuracy of procalcitonin for sepsis diagnosis in critically ill patients: systematic review and meta-analysis, Lancet Infect. Dis. 7 (2007) 210–217, https://doi.org/10.1016/S1473-3099(07)70052-X.

[11] A. Dahaba, B. Hagara, A. Fall, P. Rehak, W. List, H. Metzler, Procalcitonin for early prediction of survival outcome in postoperative critically ill patients with severe sepsis, Br. J. Addiction: Br. J. Anaesth. 97 (2006) 503–508, https://doi.org/10.1093/bja/ael181.

[12] J.M. Lim, M.Y. Ryu, J.H. Kim, C.H. Cho, T.J. Park, J.P. Park, An electrochemical biosensor for detection of the sepsis-related biomarker procalcitonin, RSC Adv. 7 (2017) 36562–36565, https://doi.org/10.1039/C7RA06553A.

[13] A. Munack, CIGR "Handbook of Agricultural Engineering", Volume VI–Information Technology, ASABE Publication, 2006.

[14] X. Tang, S. Bansaruntip, N. Nakayama, E. Yenilmez, Y.-l. Chang, Q. Wang, Carbon nanotube DNA sensor and sensing mechanism, Nano Lett. 6 (2006) 1632–1636, https://doi.org/10.1021/nl060613v.

[15] R. Mukhopadhyay, V.V. Sumbayev, M. Lorentzen, J. Kjems, P.A. Andreasen, F. Besenbacher, Cantilever sensor for nanomechanical detection of specific protein conformations, Nano Lett. 5 (2005) 2385–2388, https://doi.org/10.1021/nl051449z.

[16] J. Wang, G. Rivas, X. Cai, E. Palecek, P. Nielsen, H. Shiraishi, N. Dontha, D. Luo, C. Parrado, M. Chicharro, DNA electrochemical biosensors for environmental monitoring. A review, Anal. Chim. Acta 347 (1997) 1–8, https://doi.org/10.1016/S0003-2670(96)00598-3.

[17] G. Liu, Y. Wan, V. Gau, J. Zhang, L. Wang, S. Song, C. Fan, An enzyme-based E-DNA sensor for sequence-specific detection of femtomolar DNA targets, J. Am. Chem. Soc. 130 (2008) 6820–6825, https://doi.org/10.1021/ja800554t.

[18] M.J. Lobo, A.J. Miranda, P. Tuñón, Amperometric biosensors based on NAD (P)-dependent dehydrogenase enzymes, Electroanalysis 9 (1997) 191–202, https://doi.org/10.1002/elan.1140090302.

[19] Y. Zhang, S. Tadigadapa, Calorimetric biosensors with integrated microfluidic channels, Biosens. Bioelectron. 19 (2004) 1733–1743, https://doi.org/10.1016/j.bios.2004.01.009.

[20] B. Zhang, T. Cui, An ultrasensitive and low-cost graphene sensor based on layer-by-layer nano self-assembly, Appl. Phys. Lett. 98 (2011), 073116, https://doi.org/10.1063/1.3557504.

[21] O.S. Kwon, S.J. Park, J.-Y. Hong, A.-R. Han, J.S. Lee, J.S. Lee, J.H. Oh, J. Jang, Flexible FET-type VEGF aptasensor based on nitrogen-doped graphene converted from conducting polymer, ACS Nano 6 (2012) 1486–1493, https://doi.org/10.1021/nn204395n.

[22] Y.H. Kwak, D.S. Choi, Y.N. Kim, H. Kim, D.H. Yoon, S.-S. Ahn, J.-W. Yang, W. S. Yang, S. Seo, Flexible glucose sensor using CVD-grown graphene-based field effect transistor, Biosens. Bioelectron. 37 (2012) 82–87, https://doi.org/10.1016/j.bios.2012.04.042.

[23] Y. Huang, X. Dong, Y. Liu, L.-J. Li, P. Chen, Graphene-based biosensors for detection of bacteria and their metabolic activities, J. Mater. Chem. 21 (2011) 12358–12362, https://doi.org/10.1039/C1JM11436K.

[24] W. Yang, K.R. Ratinac, S.P. Ringer, P. Thordarson, J.J. Gooding, F. Braet, Carbon nanomaterials in biosensors: should you use nanotubes or graphene, Angew. Chem. Int. Ed. 49 (2010) 2114–2138, https://doi.org/10.1002/anie.200903463.

[25] M.S. Mannoor, H. Tao, J.D. Clayton, A. Sengupta, D.L. Kaplan, R.R. Naik, N. Verma, F.G. Omenetto, M.C. McAlpine, Graphene-based wireless bacteria detection on tooth enamel, Nat. Commun. 3 (2012) 1–9, https://doi.org/10.1038/ncomms1767.

[26] O. Akhavan, E. Ghaderi, A. Esfandiar, Wrapping bacteria by graphene nanosheets for isolation from environment, reactivation by sonication, and inactivation by near-infrared irradiation, J. Phys. Chem. B 115 (2011) 6279–6288, https://doi.org/10.1021/jp200686k.

[27] O. Akhavan, E. Ghaderi, Escherichia coli bacteria reduce graphene oxide to bactericidal graphene in a self-limiting manner, Carbon 50 (2012) 1853–1860, https://doi.org/10.1016/j.carbon.2011.12.035.

[28] O. Akhavan, E. Ghaderi, Toxicity of graphene and graphene oxide nanowalls against bacteria, ACS Nano 4 (2010) 5731–5736, https://doi.org/10.1021/nn101390x.

[29] Y. Tu, M. Lv, P. Xiu, T. Huynh, M. Zhang, M. Castelli, Z. Liu, Q. Huang, C. Fan, H. Fang, Destructive extraction of phospholipids from Escherichia coli membranes by graphene nanosheets, Nat. Nanotechnol. 8 (2013) 594–601, https://doi.org/10.1038/nnano.2013.125.

[30] P.K. Basu, D. Indukuri, S. Keshavan, V. Navratna, S.R.K. Vanjari, S. Raghavan, N. Bhat, Graphene based E. coli sensor on flexible acetate sheet, Sensor. Actuator. B Chem. 190 (2014) 342–347, https://doi.org/10.1016/j.snb.2013.08.080.

[31] B. Yao, Y. Wu, Y. Cheng, A. Zhang, Y. Gong, Y.-J. Rao, Z. Wang, Y. Chen, All-optical Mach–Zehnder interferometric NH3 gas sensor based on graphene/microfiber hybrid waveguide, Sensor. Actuator. B Chem. 194 (2014) 142–148, https://doi.org/10.1016/j.snb.2013.12.085.

[32] S. He, B. Song, D. Li, C. Zhu, W. Qi, Y. Wen, L. Wang, S. Song, H. Fang, C. Fan, A graphene nanoprobe for rapid, sensitive, and multicolor fluorescent DNA analysis, Adv. Funct. Mater. 20 (2010) 453–459, https://doi.org/10.1002/adfm.200901639.

[33] Y. Zhang, H. Zhao, Z. Wu, Y. Xue, X. Zhang, Y. He, X. Li, Z. Yuan, A novel graphene-DNA biosensor for selective detection of mercury ions, Biosens. Bioelectron. 48 (2013) 180–187, https://doi.org/10.1016/j.bios.2013.04.013.

[34] P. Nguyen, V. Berry, Graphene interfaced with biological cells: opportunities and challenges, J. Phys. Chem. Lett. 3 (2012) 1024–1029, https://doi.org/10.1021/jz300033g.

[35] W. Li, B. Chen, C. Meng, W. Fang, Y. Xiao, X. Li, Z. Hu, Y. Xu, L. Tong, H. Wang, Ultrafast all-optical graphene modulator, Nano Lett. 14 (2014) 955–959, https://doi.org/10.1021/nl404356t.

[36] B. Yao, Y. Wu, D. Webb, J. Zhou, Y. Rao, A. Pospori, C. Yu, Y. Gong, Y. Chen, Z. Wang, Graphene-based D-shaped polymer FBG for highly sensitive erythrocyte detection, IEEE Photon. Technol. Lett. 27 (2015) 2399–2402, https://doi.org/10.1109/LPT.2015.2466614.

[37] M.E. Ayhan, CVD graphene-based flexible and transparent SERS substrate towards L-tyrosine detection, Microelectron. Eng. 241 (2021), 111546, https://doi.org/10.1016/j.mee.2021.111546.

[38] S. Kim, S. Shin, T. Kim, H. Du, M. Song, C. Lee, K. Kim, S. Cho, D.H. Seo, S. Seo, Robust graphene wet transfer process through low molecular weight polymethylmethacrylate, Carbon 98 (2016) 352–357, https://doi.org/10.1016/j.carbon.2015.11.027.

[39] B. Gür, M.E. Ayhan, Molibden oksit, Pluronic® F127 ve mantarın lityum tetraborat/ITO elektrotların kapasitif özelliklerine etkilerinin incelenmesi, Afyon Kocatepe Üniversitesi Fen Ve Mühendislik Bilimleri Dergisi 21 (2019) 196–208, https://doi.org/10.35414/akufemubid.870456.

[40] B. Gür, Determination of the pH-dependent immobilization efficacy of α-glycosidase and its catalytic performance on SnO2: Sb/ITO thin films, Biochem. Eng. J. 163 (2020), 107758, https://doi.org/10.1016/j.bej.2020.107758.

[41] Gür. B, Ayhan. M.E, Türkhan. A, Gür. F, Kaya. E.D, A facile immobilization of polyphenol oxidase enzyme on graphene oxide and reduced graphene oxide thin films: An insight into in-vitro activity measurements and characterization. Colloids Surf. A Physicochem. Eng. Asp. 562 179–185 10.1016/j.colsurfa.2018.11.041.

[42] J. Ou, J. Wang, S. Liu, B. Mu, J. Ren, H. Wang, S. Yang, Tribology study of reduced graphene oxide sheets on silicon substrate synthesized via covalent assembly, Langmuir 26 (2010) 15830–15836, https://doi.org/10.1021/la102862d.

[43] L. Yang, J. Xue, Y. Jia, Y. Zhang, D. Wu, H. Ma, Q. Wei, H. Ju, Construction of well-ordered electrochemiluminescence sensing interface using peptide-based specific antibody immobilizer and N-(aminobutyl)-N-(ethylisoluminol) functionalized ferritin as signal indicator for procalcitonin analysis, Biosens. Bioelectron. 142 (2019), 111562, https://doi.org/10.1016/j.bios.2019.111562.

[44] M. Alam, A. Asiri, M. Rahman, Electrochemical detection of 2-nitrophenol with BaO nanorods modified glassy carbon electrode, Chem. Asian J. (2021), https://doi.org/10.1002/asia.202100250.

[45] F. Gür, E.D. Kaya, B. Gür, A. Türkhan, Y. Onganer, Preparation of bio-electrodes via Langmuir-Blodgett technique for pharmaceutical and waste industries and their biosensor application, Colloids Surf. A Physicochem. Eng. Asp. 583 (2019), 124005, https://doi.org/10.1016/j.colsurfa.2019.124005.

[46] E.B. Aydın, M. Aydın, M.K. Sezgintürk, A highly sensitive immunosensor based on ITO thin films covered by a new semi-conductive conjugated polymer for the determination of TNFα in human saliva and serum samples, Biosens. Bioelectron. 97 (2017) 169–176, https://doi.org/10.1016/j.bios.2017.05.056.

[47] F. Parnianchi, S. Kashanian, M. Nazari, M. Peacock, K. Omidfar, K. Varmira, Ultrasensitive electrochemical sensor based on molecular imprinted polymer and ferromagnetic nanocomposite for bilirubin analysis in the saliva and serum of newborns, Microchem. J. 179 (2022), 107474, https://doi.org/10.1016/j.microc.2022.107474.

[48] Y.S. Grewal, M.J. Shiddiky, L.J. Spadafora, G.A. Cangelosi, M. Trau, Nano-yeast–scFv probes on screen-printed gold electrodes for detection of Entamoeba histolytica antigens in a biological matrix, Biosens. Bioelectron. 55 (2014) 417–422.

[49] T. Bayraktutan, B. Gür, Y. Onganer, A new FRET-based functional chemosensor for fluorometric detection of Fe3+and its validation through in silico studies, J. Mol. Struct. 1256 (2022), 132448, https://doi.org/10.1016/j.molstruc.2022.132448.

[50] Y. Huang, M.C. Bell, I.I. Suni, Impedance biosensor for peanut protein Ara h 1, Anal. Chem. 80 (23) (2008) 9157–9161.

[51] A. Lasia, Electrochemical Impedance Spectroscopy and its Applications, Modern Aspects of Electrochemistry, 2014. Springer.

[52] E. Katz, I. Willner, Probing biomolecular interactions at conductive and semiconductive surfaces by impedance spectroscopy: routes to impedimetric immunosensors, DNA-sensors, and enzyme biosensors, Electroanalysis: An International Journal Devoted to Fundamental and Practical Aspects of Electroanalysis 15 (11) (2003) 913–947.

[53] I.I. Suni, Impedance methods for electrochemical sensors using nanomaterials, TrAC, Trends Anal. Chem. 27 (7) (2008) 604–611.

[54] N. Aydemir, J. Malmström, J. Travas-Sejdic, Conducting polymer based electrochemical biosensors, Phys. Chem. Chem. Phys. 18 (2016) 8264–8277, https://doi.org/10.1039/C5CP06830D.

[55] F.J. Wiedermann, N. Kaneider, P. Egger, W. Tiefenthaler, C.J. Wiedermann, K. H. Lindner, W. Schobersberger, Migration of human monocytes in response to procalcitonin, Crit. Care Med. 30 (2002) 1112–1117, https://doi.org/10.1097/01.CCM.0000134404.63292.71.

[56] P. Schuetz, W. Albrich, B. Mueller, Procalcitonin for diagnosis of infection and guide to antibiotic decisions: past, present and future, BMC Med. 9 (2011) 1–9. http://www.biomedcentral.com/1741-7015/9/107.

[57] D. Gendrel, J. Raymond, M. Assicot, F. Moulin, J.-L. Iniguez, P. Lebon, C. Bohuon, Measurement of procalcitonin levels in children with bacterial or viral meningitis, Clin. Infect. Dis. 24 (1997) 1240–1242, https://doi.org/10.1086/513633.

[58] Y. van der Does, M. Limper, K.E. Jie, S.C.E. Schuit, H. Jansen, N. Pernot, J. van Rosmalen, M.J. Poley, C. Ramakers, P. Patka, E.C.M. van Gorp, P.P.M. Rood, Procalcitonin-guided antibiotic therapy in patients with fever in a general emergency department population: a multicentre non-inferiority randomized clinical trial (HiTEMP study), Clin. Microbiol. Infect. 24 (2018) 1282–1289, https://doi.org/10.1016/j.cmi.2018.05.011.

[59] F. Bloos, K. Reinhart, Rapid diagnosis of sepsis, Virulence 5 (2014) 154–160, https://doi.org/10.4161/viru.27393.

[60] J.Q. Liu, L. Quan, X.L. Yu, L. Wang, Quantitative detection of procalcitonin using an electrochemical immunosensor based on MoO3/Au@rGO nanocomposites, Analyst 144 (2019) 6968–6974, https://doi.org/10.1039/C9AN01721F.

[61] Z.H. Yang, Y. Zhuo, R. Yuan, Y.Q. Chai, Electrochemical activity and electrocatalytic property of cobalt phthalocyanine nanoparticles-based immunosensor for sensitive detection of procalcitonin, Sensor. Actuator. B Chem. 227 (2016) 212–219, https://doi.org/10.1016/j.snb.2015.08.109.

[62] X. Xu, X. Li, J. Sensors, B-Chemical Miao Actuators, L. Liu, X. Huang, Q. Wei, W. Cao, A dual-mode label-free electrochemical immunosensor for ultrasensitive detection of procalcitonin based on gC 3 N 4-NiCo 2 S 4-CNTs-Ag NPs, Analyst 146 (2021) 3169–3176, https://doi.org/10.1039/D1AN00372K.

[63] Y. Li, W. Liu, G. Jin, Y. Niu, Y. Chen, M. Xie, Label-free sandwich imaging ellipsometry immunosensor for serological detection of procalcitonin, Anal. Chem. 90 (2018) 8002–8010, https://doi.org/10.1021/acs.analchem.8b00888.

[64] G. Wang, Y. Wan, G. Lin, Z. Li, Z. Dong, T. Liu, Development of a novel chemiluminescence immunoassay for the detection of procalcitonin, J. Immunol. Methods 484–485 (2020), 112829, https://doi.org/10.1016/j.jim.2020.112829.